Chaos, Solitons and Fractals 185 (2024) 115129

Contents lists available at ScienceDirect

Chaos, Solitons and Fractals

journal homepage: www.elsevier.com/locate/chaos

Percolation-induced explosive synchronization in pinning control

Camilla Ancona [a], Fabio Della Rossa [b], Francesco Lo Iudice [a,*], Pietro De Lellis [a,*]

[a] Department of Electrical Engineering and Information Technology, University of Naples Federico II, via Claudio 21, Naples 80125, Italy
[b] Department of Electronics, Information, and Bioengineering, Politecnico di Milano, Milan 20133, Italy

ARTICLE INFO

Keywords:
Complex networks
Percolation
Phase transition
Pinning control
Synchronization

ABSTRACT

Percolation and synchronization are two paradigmatic examples of phase transitions that can take place in network dynamical systems. In this paper, we show how percolation can induce an explosive, first-order transition to synchronization in pinning control, a classical feedback strategy that exploits the network topology to drive the network dynamics to a desired synchronous solution. When the number of control signals is limited by physical or economical constraints, only a fraction of the network nodes can be effectively synchronized onto the desired trajectory. Determining the sensitivity of this fraction to the number of pinning control signals is then key to decide if it is worth adding additional control signals. We find that when the network graph percolates, that is, it becomes endowed with a giant strongly connected component (G_{SCC}), an explosive transition to synchronization occurs as we increase the fraction of nodes where we can inject the pinning signals. Motivated by this numerical observation, we exploit the probabilistic conditions that ensure the presence of a G_{SCC} to predict the number of pinning signals such that all of its nodes will converge to the desired synchronous trajectory. We test the validity and robustness of our analytical derivations through numerical simulations on both synthetic and real networks, proving the benefit of such analysis in supporting decision-making for control design.

1. Introduction

In the last decades, the complex networks paradigm has risen as the tool of choice to model real world systems made of interacting agents [1]. As the ability to model, analyze, and design interventions on these systems requires combining tools from statistical mechanics, nonlinear dynamics, and control theory, research on complex networks has attracted joint efforts by physicists, applied mathematicians, and control engineers [2–4]. The overarching goal in studying the dynamics of network systems has been that of linking the emergence of collective phenomena with the structure of interaction network and the individual dynamics of the nodes [5]. For example, in [6], the authors study the emergence of traffic jams for different selections of the routing protocol. A critical problem in studying the onset of a collective behavior is understanding whether the transition from an incoherent to a coherent network behavior is abrupt or smooth. In an analogy with thermodynamics, the former is deemed as a first-order phase transition (discontinuous and irreversible), while the latter a second-order phase transition (continuous and reversible) [7–9].

When the collective behavior under analysis is synchronization, a classical model to study its emergence considers a network of N dynamical systems over a digraph $\mathcal{G}$, whose dynamics can be written as

$$\dot{x}_i = f(x_i, t) + c \sum_{j=1}^{N} a_{ij} \tilde{h}(x_i, x_j), \quad i = 1, \dots, N, \tag{1}$$

where $x_i \in \mathbb{R}^n$ is the state of the ith node, c is the coupling strength between neighboring nodes, a_{ij} the entry ij of the adjacency matrix associated to $\mathcal{G}$, the vector field $f : \mathbb{R}^n \times \mathbb{R}_{\geq 0} \to \mathbb{R}^n$ describes the nodal intrinsic dynamics, and $\tilde{h} : \mathbb{R}^n \times \mathbb{R}^n \to \mathbb{R}^n$ is the coupling function. We study the onset of collective behaviors in network (1) under the assumption that the coupling function $\tilde{h}$ can be written as a function of the state difference between neighboring nodes, that is,

$$\tilde{h}(x_i, x_j) = h(x_j - x_i),$$

where $h : \mathbb{R}^n \to \mathbb{R}^n$.

In synchronization problems, the transition to coherent oscillatory dynamics is typically regulated by the coupling strength c, see e.g. [10–12]. In this scenario, a second-order phase transition usually occurs [11], albeit first-order transitions have been observed in the presence of specific coupling configurations and individual dynamics [12,13]. However, synchronization does not always emerge

* Corresponding authors.
E-mail addresses: camilla.ancona2@unina.it (C. Ancona), fabio.dellarossa@polimi.it (F. Della Rossa), francesco.loiudice2@unina.it (F. Lo Iudice), pietro.delellis@unina.it (P. De Lellis).

https://doi.org/10.1016/j.chaos.2024.115129
Received 26 March 2024; Received in revised form 10 May 2024; Accepted 3 June 2024
Available online 10 June 2024

spontaneously, but may also be induced by the injection of control signals, modeled as an additional term in the right-hand side of (1), see e.g. [14,15] and references therein. In [16], the authors identified the minimum driver node selection that makes the network structurally controllable.

A classical control strategy that aims at steering the nodes of a complex network towards a desired solution $s(t)$ of the individual dynamics is pinning control, which prescribes to exert a proportional feedback control action on a limited number of network nodes, the *pinned* nodes $\mathcal{P}$ [17,18]. In the presence of this external control action, the dynamics of the ith node modifies as

$$\dot{x}_i = f(x_i, t) + c \sum_{j=1}^{N} a_{ij} h(x_j - x_i) - \kappa \delta_i h(x_i - s), \tag{2a}$$

$$\sum_{i=1}^{N} \delta_i = m, \tag{2b}$$

where the binary variable δ_i is one only if node i is pinned, κ is the control gain modulating the strength of the control action, and constraint (2b) sets the allowed number of pinned nodes to m, that is, $|\mathcal{P}| = m$.

In the presence of a pinning control action, then two factors, in addition to the coupling strength c, regulate the transition to the desired synchronous solution: the control gain κ, and the selection of the nodes where the control signals are injected, that is, the choice of $\delta_1, \dots, \delta_N$. In [19], the authors showed that, given that c and κ are sufficiently large, and that the vector field f fulfills the so-called QUAD condition[1] [21], the selection of the pinned nodes (i.e., of the non-zero δ_i-s) determines the extent to which a network synchronizes, that is, the set of nodes $\mathcal{Q}$ that converge to the reference trajectory $s(t)$. Furthermore, they proposed an algorithm to maximize the number of nodes that achieve synchronization (i.e., the cardinality of $\mathcal{Q}$), given the number m of pinned nodes.

Under the assumption that the individual dynamics fulfill the QUAD condition [21], the application of the algorithm in [19] to the controlled network system (2) for all possible values of m allows then to discriminate the type of transition to synchronization. In Fig. 1, the fraction of controlled nodes $|\mathcal{Q}|/N$ is shown as a function of the number of pinned nodes m for two different graph topologies, one reconstructed from Facebook friendships and the other from the network of scientific collaborations [22]. The two different graph topologies induce two different transitions to synchronization: first-order for the Facebook friendship network, and second-order for the network of scientific collaborations. The main difference between the two network topologies is that only the first is endowed of a giant strongly connected component G_{SCC}. This observation suggests that the presence of a G_{SCC}, whose development is the result of a percolation, determines an explosive phase transition in the fraction of nodes that we are able to control as we increase the number of pinned nodes. In this paper, we call this phenomenon percolation-induced explosive synchronization, and explore how we can detect its emergence. The knowledge of the type of transition occurring in (2) would be indeed paramount for control design. In taking the decision of adding more control signals, one may expect proportional gains in the fraction of nodes that we are able to control. This is, however, far from true in a first-order transition, in which adding further control signals may be worth only if it implies overcoming the critical threshold for the transition to take place.

In this work, we show that the algorithm in [19] can be extended to a wider class of network systems, whose individual dynamics may not fulfill the QUAD condition. In principle, the algorithm could then be extensively utilized by varying the fraction of controlled nodes to determine whether a first- or second-order transition takes place. Unfortunately, the computational cost of detecting the phase transition type, and the tipping point in case of first-order transitions, through the algorithm in [19] is as high as the value of information they would bring to the control designer, since it would require solving a (large) sequence of combinatorial NP-hard optimization problems.

These considerations prompted us to attempt estimating the main features of the phase transition that takes place as we increase the number of nodes we can pin, without the necessity of solving the algorithm in [19]. In particular, we leveraged the properties of the generating functions to derive this estimation solely based on the knowledge of the degree distribution of the network we are aiming to control.

The outline of the manuscript is as follows. In Section 2, we generalize the results on pinning control provided in [19] to a wider class of coupled dynamical systems, extending the definition of type II master stability function provided e.g. in [1,23]. We then use this result to show that, when a giant component is present, the phase transition in the number of controllable nodes is explosive. In Section 3, we then focus on the case in which an explosive transition takes place. Namely, we derive an analytical prediction of the critical fraction of controlled nodes triggering the transition, and we provide a lower and upper bound for the number of nodes that we can control as the transition takes place. In Section 4, we then gauge the accuracy of our estimate on both real and synthetic datasets. Finally, we draw the conclusions and outline future research avenues in Section 5.

2. Linking phase transitions in pinning controlled nodes with network topology

2.1. Digraphs and their condensation graph

A digraph $\mathcal{G}$ is described by the pair $(\mathcal{V}_\mathcal{G}, \mathcal{E}_\mathcal{G})$, where $\mathcal{V}_\mathcal{G}$ is the set of its nodes, and $\mathcal{E}_\mathcal{G}$ is the set of its edges, defined as ordered pairs of nodes. Given two nodes $i, j \in \mathcal{V}_\mathcal{G}$, i is reachable from j if there exists a directed path from j to i. For a given node i, we define the node in-degree $k_{\mathrm{in}}(i)$ and out-degree $k_{\mathrm{out}}(i)$ as the number of edges coming in and going out from node i, respectively.

Given a subset of nodes $\mathcal{N} \subset \mathcal{V}_\mathcal{G}$, the downstream $\mathcal{D}(\mathcal{N})$ of $\mathcal{N}$ is the set of nodes reachable from a node in $\mathcal{N}$, whereas its upstream $\mathcal{U}(\mathcal{N})$ is the set of nodes from which a node in $\mathcal{N}$ is reachable. Note that, from this definition $\mathcal{N} \subseteq \mathcal{U}(\mathcal{N})$, $\mathcal{N} \subseteq \mathcal{D}(\mathcal{N})$, and $\mathcal{N} = \mathcal{U}(\mathcal{N}) \cap \mathcal{D}(\mathcal{N})$.

A strongly connected component (SCC) of a digraph $\mathcal{G}$ is a strongly connected subgraph $\mathcal{S}(\mathcal{G})$ of $\mathcal{G}$ such that any other subgraph $\mathcal{S}'(\mathcal{G})$ strictly containing $\mathcal{S}(\mathcal{G})$ is not strongly connected. Any graph $\mathcal{G}$ has $p \geq 1$ SCCs, which we denote $\mathcal{G}_i$, $i = 1, \dots, p$. With a slight abuse of notation, we will denote $\mathcal{V}_i$ and $\mathcal{E}_i$ the node and edge sets of $\mathcal{G}_i$, respectively.

The condensation of $\mathcal{G}$ is the directed acyclic graph $\mathcal{G}^D = \{\mathcal{V}^D, \mathcal{E}^D\}$, whose nodes are the SCCs of $\mathcal{G}$, and whose edges represent the inter-SCC connections. Namely, the existence of at least an edge $(l, m) \in \mathcal{E}^D$ means that there is an edge from a node i in the lth SCC of $\mathcal{G}$ to a node j in the mth SCC of $\mathcal{G}$. A SCC that does not have any inbounding edge (that is, a node of the condensation graph with zero in-degree) is called a root strongly connected component (R_{SCC}) of $\mathcal{G}$.

2.2. Pinning control of digraphs and the special role of the R_{SCC}-s

Let us consider the hth SCC, and let us identify the pinner node, which injects the control signal, as the node $N+1$, with state $x_{N+1}(t) = s(t)$. We then define an extended adjacency matrix A_{ext}, which includes the pinner, and can be written as

$$A_{\mathrm{ext}} = \begin{bmatrix} A & \gamma\delta \\ 0_N^{\mathrm{T}} & 0 \end{bmatrix}, \tag{3}$$

where $\delta = [\delta_1, \dots, \delta_N]^{\mathrm{T}}$ is a binary vector that indicates the nodes that are receiving the control signal, and $\gamma = \kappa/c$ is the ratio between the

[1] The QUAD condition, first introduced in [20], is a generalization of the one-side Lipschitz condition that defines a space of functions that can be upper bounded by a linear function.

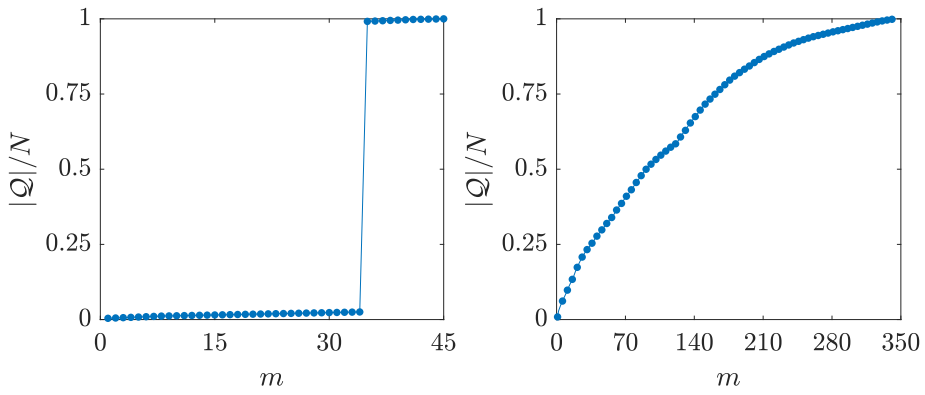

Fig. 1. Different transitions to synchronization in the controlled network systems (2) on real-world topologies when dynamics and inner coupling function fulfill the condition in [19]. The plots report the normalized number of controlled nodes $|\mathcal{Q}|/N$ as a function of the number of control inputs deployed, m. The left panel depicts the first-order phase transition occurring when the coupling topology is a digraph retrieved from Facebook [22] that is endowed of a G_{SCC}, whereby $|\mathcal{Q}|/N$ abruptly increases when m reaches 45. The right panel depicts a second-order phase transition where the coupling topology is given by a digraph describing a network of scientific collaboration [22] that is not endowed with a G_{SCC}, whereby $|\mathcal{Q}|/N$ smoothly increases with m.

control and coupling gains. Denoting $c_h = |\mathcal{U}(\mathcal{V}_h)|$, we then consider a permutation P that relabels as $1,\dots,c_h$ the nodes in the upstream of $\mathcal{V}_h$, and as c_h+1 the node corresponding to the pinner. Then, $\widetilde{A} = P^{\mathrm{T}} A_{\mathrm{ext}} P$ will be the adjacency matrix obtained through this node relabeling. From the definition of upstream, $\widetilde{A}$ is block-triangular, and can be decomposed as

$$\widetilde{A} = \begin{bmatrix} R & 0_{c_h+1,N-c_h} \\ S & W \end{bmatrix}, \tag{4}$$

where $R \in \mathbb{R}^{(c_h+1)\times(c_h+1)}$, $S \in \mathbb{R}^{(N-c_h)\times(c_h+1)}$, and $W \in \mathbb{R}^{(N-c_h)\times(N-c_h)}$. Considering that the pinner has the same dynamics as the rest of the network, once we have sorted the nodes according to the permutation matrix P, we can then rewrite the dynamics of the nodes in the upstream of $\mathcal{V}_h$ and of the pinner as

$$\dot{x}_i = f(x_i,t) + c\sum_{j=1}^{c_h+1} r_{ij} h(x_j - x_i), \quad i = 1,\dots,c_h+1, \tag{5}$$

where r_{ij} is the entry ij of R. The coupling term in (5) vanishes at the synchronization manifold $x_i = s$ for all $i = 1,\dots,c_h$, which, since the pinner's trajectory $s(t)$ is a solution of the individual dynamics, is invariant. We can then define $\delta x_i = x_i - s$ as the deviation of the ith node from s, and linearizing about the synchronous solution we obtain

$$\delta\dot{x}_i = \mathrm{JF}(s)\delta x_i - c\sum_{j=1}^{c_h+1} L^h_{ij}\mathrm{JH}(0)\delta x_j. \tag{6}$$

where $\mathrm{JF} \in \mathbb{R}^{n\times n}, \mathrm{JH} \in \mathbb{R}^{n\times n}$ are the Jacobian matrices associated with f and h, respectively, while L^h_{ij} is the entry ij of the Laplacian matrix $L^h \in \mathbb{R}^{(c_h+1)\times(c_h+1)}$ associated to R, and we omit for brevity the explicit dependence on time.

In what follows, we assume that at least one node in each R_{SCC} in $\mathcal{U}(\mathcal{V}_h)$ is pinned. This is a necessary and sufficient condition for the subgraph defined by the nodes in $\mathcal{U}(\mathcal{V}_h)$ to encompass a spanning tree originating from the node associated to the pinner, and equivalently, a necessary and sufficient condition for the eigenvalue 0 of L^h to be simple. In what follows, we denote by $\lambda_1 = 0$ the simple 0 eigenvalue of L^h, and by λ_i, $i = 2,\dots,c_h+1$ its remaining eigenvalues, all with positive real part.

Defining the vector $\delta x = \left[\delta x_1;\dots;\delta x_{c_h+1}\right]$, and the matrix V such that $V^{-1}L^hV$ is in Jordan form, we can then introduce the transformation $\eta = \left(V^{-1}\otimes I_n\right)\delta x$ whose components are $\left[\eta_1;\dots;\eta_{c_h+1}\right]$, where $\eta_i \in \mathbb{R}^n$.

From (6), the dynamics along the synchronization manifold will be described by $\dot{\eta}_1 = \mathrm{JF}(s)\eta_1$. To study synchronizability, we then focus on the remaining blocks of the Jordan canonical form [24,25]. Given an eigenvalue $\lambda \in \mathrm{spec}(L^h)\setminus\{\lambda_1\}$, let us denote $\mu_A(\lambda)$ and $\mu_G(\lambda)$ its algebraic and geometric multiplicity, respectively. The Jordan block associated to λ will have size $b_i = 1+\mu_A(\lambda)-\mu_G(\lambda)$ and will be associated with the transformed variables $\eta_i,\dots,\eta_{i+b_i-1}$, whose dynamics are

$$\begin{aligned}
\dot{\eta}_i &= (\mathrm{JF}(s) - c\lambda\mathrm{JH}(0))\,\eta_i,\\
\dot{\eta}_{i+1} &= (\mathrm{JF}(s) - c\lambda\mathrm{JH}(0))\,\eta_{i+1} - \mathrm{JH}(0)\eta_i,\\
&\vdots\\
\dot{\eta}_{i+b_i-1} &= (\mathrm{JF}(s) - c\lambda\mathrm{JH}(0))\,\eta_{i+b_i-1} - \mathrm{JH}(0)\eta_{i+b_i-2}.
\end{aligned}$$

Introducing the master equation

$$\dot{\zeta} = (\mathrm{JF}(s) - \nu\mathrm{JH}(0))\zeta, \tag{7}$$

where $\zeta \in \mathbb{R}^n$, and $\nu \in \mathbb{C}^n$, then the maximum Lyapunov exponent $\Lambda(\nu)$ associated with (7) is the master stability function for network (5). Hence, if

$$\Lambda^h_{\max}(c) = \max_{i=2,\dots,c_h+1} \Lambda\left(c\lambda_i\right) < 0, \tag{8}$$

then all the Jordan blocks will be asymptotically stable. Therefore, the synchronization manifold of (5) will be locally asymptotically stable, thereby meaning that all nodes in the upstream of the hth SCC will converge onto the pinner's trajectory.

Remark 1. Note that the same derivations could be performed also when the coupling function in (1) is selected as $\tilde{h}(x_i,x_j) = h(x_i) - h(x_j)$ instead of $\tilde{h}(x_i,x_j) = h(x_i - x_j)$. The only difference would be that the Jacobian of h should be computed at s rather than at 0, and therefore in all equations from (6) to (7) JH(0) should be replaced by JH(s).

The fulfillment of (8) depends on the coupling gain c and on the eigenvalues of L^h, which in turn depend on the topology of the upstream of the hth SCC, and on the ratio γ between the control and coupling gain. Therefore, for a given network topology and a given γ, $\Lambda^h_{\max}$ will only depend on c. Starting from the classification first given in [1] and then extended to higher-order interactions in [23,26], we extend the definition of type II master stability function to the case of a pinning controlled network.

Definition 1. Given the controlled network dynamical system (2), the master stability function associated to it is of type II if for all topologies such that the 0 eigenvalue of the Laplacian L^h is simple, and for all $\gamma > 0$, there exists a threshold $\bar{c}(\gamma, L^h)$ such that the master stability function is negative for all $c > \bar{c}(\gamma, L^h)$.

An immediate consequence of the above definition is the following proposition:

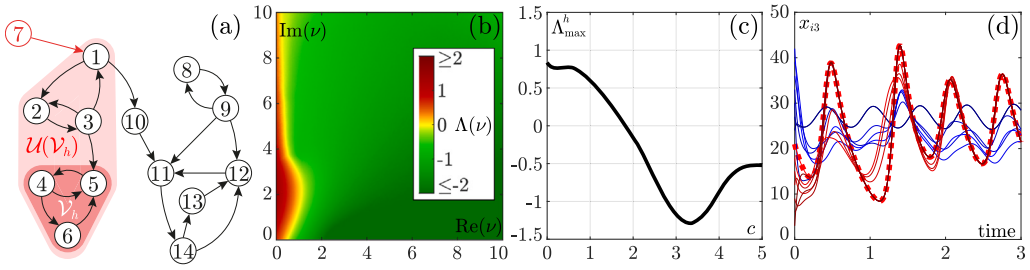

Fig. 2. Example of application of Proposition 1. Panel (a) depicts the network topology; each node is a Lorenz oscillator, whereby in (5) we set $f = [10(x_{i2} - x_{i1});\ x_{i1}(28 - x_{i3}) - x_{i2};\ x_{i1}x_{i2} - 8/3x_{i3}]$, whereas the coupling function is set to $h(x) = x$. We focus on controlling the SCC $\mathcal{V}_h = \{4, 5, 6\}$, shaded in red, whose upstream $\mathcal{U}(\mathcal{V}_h)$ is shaded in pink and composed by $c_h = 6$ nodes. To control $\mathcal{V}_h$, we add the pinner node ($c_h + 1 = 7$, in red) that directly controls one of the nodes in the sole R_{SCC} of $\mathcal{U}(\mathcal{V}_h)$, that is, node 1 in $\mathcal{V}_1 = \{1, 2, 3\}$. We set the ratio γ to 1, and are free to suitably tune the coupling gain c. Panel (b) depicts a colormap of the master stability function $\Lambda(\nu)$ as a function of the complex parameter ν. Panel (c) depicts the function $\Lambda^h_{\max}$ as a function of the coupling gain c for the network in panel (a). In panel (d) we report the dynamics of the third state variable of each node $x_{i3}(t)$ when c is set to 3 so that $\Lambda^h_{\max}(c) < 0$; the trajectories of the nodes in $\mathcal{U}(\mathcal{V}_h)$ are depicted in red, and the trajectory of the pinner is dotted. The trajectories of the remaining nodes are depicted in blue. (For interpretation of the references to color in this figure legend, the reader is referred to the web version of this article.)

Proposition 1. *Let the controlled network dynamical system (2) have a type II master stability function according to Definition 1. Then, for any $\gamma > 0$, if at least one node in each R_{SCC} of $\mathcal{U}(\mathcal{V}_h)$ is pinned, and $c > \bar{c}(\gamma, L^h)$, then all nodes in $\mathcal{U}(\mathcal{V}_h)$ are locally pinning controlled.*

Proof. As at least one node in each R_{SCC} of $\mathcal{U}(\mathcal{V}_h)$ is pinned, the Laplacian L^h will have a simple 0 eigenvalue. From Definition 1, we then have that, for all $c > \bar{c}(\gamma, L^h)$, $\Lambda^h_{\max}$ is negative, and thus the thesis follows. □

Remark 2. Note that the class of controlled network systems with a type II master stability function is wider than the class of systems that can be globally pinning controlled according to [19]. Indeed, all systems in [19] will have a negative master stability function beyond a certain threshold, otherwise the necessary condition for pinning control would not be fulfilled. On the other hand, the conditions in [19] only include QUAD dynamical systems, whereas type II master stability functions can be also exhibited by non-QUAD dynamical systems, such as the Lorenz system, as illustrated in Fig. 2.

The application of the result illustrated in Proposition 1 to the entire network (2) implies that, if the coupling and control gains c and κ are large enough, the nodes of an SCC will synchronize only if at least one node in each R_{SCC} of its upstream is pinned, whereas none will synchronize otherwise. This result then explains the role played by the G_{SCC} in determining the onset of an explosive transition in the number of nodes controlled to the pinner's trajectory. Fig. 3 illustrates the classic decomposition of a graph endowed with a G_{SCC}, where the upstream and downstream of the G_{SCC} corresponds to the giant in- and out-components G_{IN} and G_{OUT}, respectively, according to the standard illustration in [27]. When the number of pinned nodes m reaches the number $m^\star$ of roots in G_{IN}, this triggers an explosive first-order phase transition in the number of controllable nodes. Indeed, the G_{SCC} encompasses most of the network nodes (except when the average network degree is very small) and, by pinning one node in each root of the G_{IN}, we can pinning control all nodes in G_{IN}, plus the remaining SCCs that have an upstream whose R_{SCC}-s are contained in G_{IN}. Therefore, when the number of pinned nodes reaches $m^\star$, the number of pinning controllable nodes will be lower bounded by the size of G_{IN}, abruptly switching from being negligible to being the majority of the network nodes.

3. Predicting the onset of an explosive phase transition from degree distribution

According to the above considerations, when the network topology is known, the SCCs of a graph can be identified by using the Tarjan's algorithm [28], so that the presence of the G_{SCC} can be detected, and the critical threshold $m^\star$ triggering the explosive transition to synchronization be computed by using the algorithm in [19]. However, this path cannot be followed when the network topology is unknown.

Next, we consider the case in which we are only aware of the network joint in- and out-degree distribution $P(k_{\text{in}}, k_{\text{out}})$, that is, the probability that a randomly chosen node has in-degree k_{in} and out-degree k_{out}, and, based on this information, we will try to predict the type of phase transition that occurs when increasing the number of pinning controllable nodes and, if an explosive one is expected, the threshold $m^\star$ that triggers the transition.

As we discussed in Section 2.2, when the network control system has a type II master stability function, the nodes of the G_{SCC} will be pinning controllable only if at least one node in each R_{SCC} is pinned. Therefore, the problem of predicting the onset of an explosive transition can be translated into the problem of estimating the number of R_{SCC}-s in the upstream of the G_{SCC}. To perform this estimate, we first approximate the number of R_{SCC}-s to the number of nodes belonging to the in-giant component with in-degree zero, and then estimate how many of these will be roots of the upstream of G_{SCC}.

In deriving our estimates, we shall use the results on the joint in- and out-degree distribution that hold for infinite size networks, and then we will test the accuracy of the estimations on finite-size network topologies.

To this aim, we introduce the generating function $\Phi(x, y) = \sum_{k_{\text{in}}, k_{\text{out}}} P(k_{\text{in}}, k_{\text{out}}) x^{k_{\text{in}}} y^{k_{\text{out}}}$, where x and y are two scalars such that $|x| \leq 1$ and $|y| \leq 1$, thus guaranteeing the convergence of the series [29,30]. As illustrated in [27], denoting $\bar{k} := \partial_x \Phi(x, 1)\big|_{x=1} = \partial_y \Phi(1, y)\big|_{y=1}$ the average in- and out-degree of the network, the giant strongly connected component is present if

$$\frac{\partial^2_{xy} \Phi(x, y)|_{x=y=1}}{\bar{k}} = \frac{\sum_{k_{\text{in}}, k_{\text{out}}} k_{\text{in}} k_{\text{out}} P(k_{\text{in}}, k_{\text{out}})}{\bar{k}} > 1,$$

or, equivalently, if

$$\bar{k} + \frac{\mathrm{E}[(k_{\text{in}} - \bar{k})(k_{\text{out}} - \bar{k})]}{\bar{k}} > 1. \tag{9}$$

Eq. (9) implies that for networks with uncorrelated in- and out-degree distributions the existence of the G_{SCC} is expected when the average degree $\bar{k}$ is greater than one. As discussed in Section 2.2, as the presence of the G_{SCC} implies an explosive pinning synchronizability of the network, the fulfillment of (9) determines whether such an explosive phase transition will occur.

Next, we define $\Phi_1^{\text{in}}(x) = \frac{\partial_y \Phi(x,y)\big|_{y=1}}{\bar{k}}$ and $\Phi_1^{\text{out}}(y) = \frac{\partial_x \Phi(x,y)|_{x=1}}{\bar{k}}$. Then, we introduce the scalars x_c and y_c such that

$$x_c = \Phi_1^{(i)}(x_c), \quad y_c = \Phi_1^{(o)}(y_c), \tag{10}$$

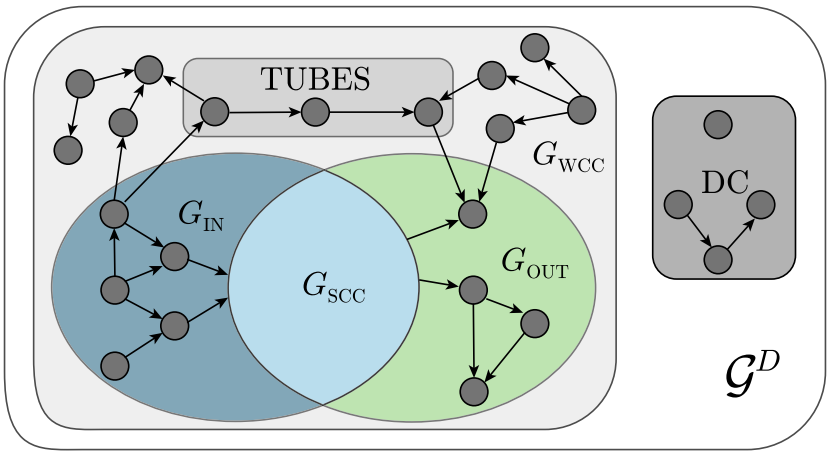

Fig. 3. Directed acyclic graph condensation of a digraph $\mathcal{G}$ endowed with a G_{SCC}. $\mathcal{G}$ is first decomposed in the giant weakly connected component G_{WCC}, which is the weakly connected component enclosing the G_{SCC}, and all remaining disconnected components DC. Within G_{WCC}, we can then identify the giant in-component G_{IN} and giant out-component G_{OUT} that correspond to the upstream and downstream of G_{SCC}, respectively, and whose intersection is G_{SCC}, and the TUBES that are the nodes not in G_{SCC} such that there is a directed path originating in G_{IN} and terminating in G_{OUT}. The remaining SCCs in G_{WCC} are called tendrils.

where x_c (y_c) can be interpreted as the probability that the strongly connected component obtained moving against (along) the edge directions, starting from a randomly chosen edge, is finite [27].

Finding x_c and y_c allows us to estimate the threshold $m^\star$, that is, the number of pinned nodes required for the onset of the phase transition. Indeed, $1-y_c^{k_{\text{out}}}$ will be the probability that a vertex whose out-degree is k_{out} has infinite components in its downstream, and $1-x_c^{k_{\text{in}}}$ the probability that a vertex with in-degree k_{in} has infinite components in its upstream. Then, the probabilities that a randomly picked node, say i, has infinite in- or out-component, that is, $P(i\in\mathcal{V}_{G_{\text{IN}}})$ and $P(i\in\mathcal{V}_{G_{\text{OUT}}})$, respectively, are

$$P(i\in\mathcal{V}_{G_{\text{IN}}})=\sum_{k_{\text{in}},k_{\text{out}}}P(k_{\text{in}},k_{\text{out}})(1-y_c^{k_{\text{out}}})=\sum_{k_{\text{out}}}P_{\text{out}}(k_{\text{out}})(1-y_c^{k_{\text{out}}}) \quad (11)$$

$$P(i\in\mathcal{V}_{G_{\text{OUT}}})=\sum_{k_{\text{in}},k_{\text{out}}}P(k_{\text{in}},k_{\text{out}})(1-x_c^{k_{\text{in}}})=\sum_{k_{\text{in}}}P_{\text{in}}(k_{\text{in}})(1-x_c^{k_{\text{in}}}), \quad (12)$$

where P_{in} and P_{out} are the marginal in- and out-degree distribution, respectively. Without any assumption on the in- and out-degree distributions, we have

$$x_c=\frac{\sum_{k_{\text{in}}}x_c^{k_{\text{in}}}\sum_{k_{\text{out}}}k_{\text{out}}P\left(k_{\text{in}},k_{\text{out}}\right)}{\bar{k}}, \quad (13)$$

$$y_c=\frac{\sum_{k_{\text{out}}}y_c^{k_{\text{out}}}\sum_{k_{\text{in}}}k_{\text{in}}P\left(k_{\text{in}},k_{\text{out}}\right)}{\bar{k}}. \quad (14)$$

Then, under the approximation that the number of network R_{SCC}-s coincides with the number of nodes with zero in-degree, the expected number m^* of R_{SCC}-s in G_{IN} can be estimated as

$$\hat{m}^\star=N\sum_{k_{\text{out}}}P\left(0,k_{\text{out}}\right)\left(1-y_c^{k_{\text{out}}}\right). \quad (15)$$

By substituting (14) in (15), one obtains

$$\hat{m}^\star=N\sum_{k_{\text{out}}}P\left(0,k_{\text{out}}\right)\left(1-\left(\frac{\sum_{k_{\text{out}}}y_c^{k_{\text{out}}}\sum_{k_{\text{in}}}k_{\text{in}}P\left(k_{\text{in}},k_{\text{out}}\right)}{\bar{k}}\right)^{k_{\text{out}}}\right). \quad (16)$$

Using Eq. (16) to estimate $m^\star$ assumes the knowledge of the joint in- and out-degree distribution. When only the marginal in- and out-distributions, denoted $P_{\text{in}}(k_i)$ and $P_{\text{out}}(k_o)$, respectively, are available, to perform the estimation one needs to assume in- and out-degrees to be independent, so that the joint distribution can be factorized. Indeed, in this case the expressions of x_c and y_c simplify as

$$x_c=\sum_{k_{\text{in}}}P_{\text{in}}\left(k_{\text{in}}\right)x^{k_{\text{in}}},\quad y_c=\sum_{k_{\text{out}}}P_{\text{out}}\left(k_{\text{out}}\right)y_c^{k_{\text{out}}},$$

since $\bar{k}=\sum_{k_{\text{out}}}k_{\text{out}}P_{\text{out}}\left(k_{\text{out}}\right)=\sum_{k_{\text{in}}}k_{\text{in}}P_{\text{in}}\left(k_{\text{in}}\right)$, and $\hat{m}^\star$ becomes

$$\begin{aligned}\hat{m}^\star&=N\sum_{k_{\text{out}}}P\left(0,k_{\text{out}}\right)\left(1-y_c^{k_{\text{out}}}\right)=NP_{\text{in}}(0)\sum_{k_{\text{out}}}P_{\text{out}}(k_{\text{out}})\left(1-y_c^{k_{\text{out}}}\right)\\&=NP_{\text{in}}(0)(1-y_c).\end{aligned} \quad (17)$$

Predicting the number of nodes in G_{WCC} that we still cannot control when the explosive transition occur.

From the results in Section 2.2, and considering the decomposition of a digraph illustrated in Fig. 3, when $m=m^\star$, the number of controllable nodes is the cardinality of the set $\mathcal{Q}(m^\star)=\mathcal{D}(\mathcal{V}_{G_{\text{IN}}})\setminus(\mathcal{D}(\text{RT}_{\text{IN}}))$, where RT_{IN} are the root strongly connected components of the tendrils from which the G_{OUT} is reachable. We denote with $\bar{\mathcal{Q}}(m^\star)$ the complement of $\mathcal{Q}(m^\star)$ with respect to $\mathcal{V}_{G_{\text{WCC}}}$, whose cardinality is the number of nodes in G_{WCC} we cannot control when the transition occurs.

In what follows, we will provide a lower and an upper bound for the probability $P(i\in\bar{\mathcal{Q}}(m^\star))$ that the generic node $i\in\mathcal{V}_{G_{\text{WCC}}}$ will not be controllable, namely $\underline{P}$ and $\overline{P}$ such that

$$\underline{P}\le P(i\in\bar{\mathcal{Q}}(m^\star))\le\overline{P}. \quad (18)$$

Once having an expression for $\underline{P}$ and $\overline{P}$, a lower and an upper bound for $|\bar{\mathcal{Q}}(m^\star)|$ can be computed by considering that $|\bar{\mathcal{Q}}(m^\star)|=P\big(i\in\bar{\mathcal{Q}}(m^\star)\big)N$.

To derive the upper bound $\overline{P}$, we can refer to the decomposition in Fig. 3 and write

$$P\big(i\in\bar{\mathcal{Q}}(m^\star)\big)\le P\big(i\in\mathcal{V}_{G_{\text{WCC}}}\big)-P\big(i\in\mathcal{V}_{G_{\text{IN}}}\big), \quad (19)$$

where the expressions for $P(i\in\mathcal{V}_{G_{\text{IN}}})$ has been given in Eq. (11); to compute $P(i\in\mathcal{V}_{G_{\text{WCC}}})$, we first recall that we can ignore the directionality in the graph when computing the probability that i belongs to G_{WCC} [30]. By introducing $\boldsymbol{\Phi}^{(w)}(x)=\boldsymbol{\Phi}(x,x)$, and denoting $\boldsymbol{\Phi}^{(w)'}$ its derivative, we calculate the scalar t_c from the implicit equation $t_c=\boldsymbol{\Phi}^{(w)'}(t_c)/2\bar{k}$. Then, $P(i\in\mathcal{V}_{G_{\text{WCC}}})$ can be computed as [27]

$$P(i\in\mathcal{V}_{G_{\text{WCC}}})=1-\frac{\boldsymbol{\Phi}^{(w)'}(t_c)}{2\bar{k}}=1-\frac{\sum_k kP_w(k)t_c^{k-1}}{2\bar{k}}, \quad (20)$$

where $k=k_{\text{in}}+k_{\text{out}}$, and $P_w(k)=\sum_{k_{\text{in}}}P(k_{\text{in}},k-k_{\text{in}})$. Putting (19), (20), (11) together, we can write

$$\overline{P}=1-\frac{\sum_k kP_w(k)t_c^{k-1}}{2\bar{k}}-\sum_{k_{\text{out}}}P_{\text{out}}(k_{\text{out}})(1-y_c^{k_{\text{out}}}). \quad (21)$$

Similarly, the fraction of nodes that are not controlled is lower bounded by the zero indegree nodes not in $\mathcal{V}_{G_{\text{IN}}} \cup \mathcal{V}_{G_{\text{OUT}}}$, that is,

$$\underline{P} = P\big((k_{\text{in}}(i) = 0) \cap i \in \mathcal{V}_{G_{\text{WCC}}} \setminus (\mathcal{V}_{G_{\text{IN}}} \cup \mathcal{V}_{G_{\text{OUT}}})\big)$$

Assuming independence yields

$$\underline{P} = P\big(k_{\text{in}}(i) = 0\big) P\big(i \in \mathcal{V}_{G_{\text{WCC}}} \setminus (\mathcal{V}_{G_{\text{IN}}} \cup V_{G_{\text{OUT}}})\big). \tag{22}$$

From the decomposition in Fig. 3, we can write

$$P\big(i \in \mathcal{V}_{G_{\text{WCC}}} \setminus (\mathcal{V}_{G_{\text{IN}}} \cup \mathcal{V}_{G_{\text{OUT}}})\big) =$$
$$P\big(i \in \mathcal{V}_{G_{\text{WCC}}}\big) - P\big(i \in \mathcal{V}_{G_{\text{IN}}}\big) - P\big(i \in \mathcal{V}_{G_{\text{OUT}}}\big) + P\big(i \in \mathcal{V}_{G_{\text{SCC}}}\big). \tag{23}$$

The expressions for $P(i \in \mathcal{V}_{G_{\text{IN}}})$ and $P(i \in \mathcal{V}_{G_{\text{OUT}}})$ has been given in Eqs. (11) and (12), respectively, whereas the probability that i belongs to the giant strongly connected component is

$$P\big(i \in \mathcal{V}_{G_{\text{SCC}}}\big) = \sum_{k_{\text{in}}} \sum_{k_{\text{out}}} P(k_{\text{in}}, k_{\text{out}})(1 - x_c^{k_{\text{in}}})(1 - y_c^{k_{\text{out}}}) \tag{24}$$

Then, substituting (11), (12), (20), (23) and (24) in (22), yields

$$\underline{P} = P_{\text{in}}(0) \left(1 - \frac{\sum_k k P_w(k) t_c^{k-1}}{2\bar{k}} - \sum_{k_{\text{out}}} P_{\text{out}}(k_{\text{out}})(1 - y_c^{k_{\text{out}}}) \right.$$
$$\left. - \sum_{k_{\text{in}}} P_{\text{in}}(k_{\text{in}})(1 - x_c^{k_{\text{in}}}) + \sum_{k_{\text{in}}, k_{\text{out}}} P(k_{\text{in}}, k_{\text{out}})(1 - x_c^{k_{\text{in}}})(1 - y_c^{k_{\text{out}}}) \right). \tag{25}$$

4. Numerical results

To test the proposed analytical prediction, we generated a collection of synthetic digraphs where we assumed the in- and out-distributions to be independent and identical, and then we considered test-bed real-world graphs, where this assumption is not necessarily met.

We assign a given degree distribution by means of the configuration model [31]. Namely, we consider two classes of degree distributions: (i) Poisson distribution $P_{\text{in}}(z) = P_{\text{out}}(z) = \frac{\lambda^z}{z!} e^{-\lambda}$ whose mean and variance both equal to λ [32], and (ii) a discretized version of the scale-free generalized Pareto distribution, with marginal probability density functions $\varphi_{\text{in}}(z) = \varphi_{\text{out}}(z) = \frac{1}{\sigma}\left(1 + \eta\frac{(z-\theta)}{\sigma}\right)^{-\frac{\eta+1}{\eta}}$ [33], where $k \neq 0$ is the shape parameter, σ is the scale parameter, and θ is the threshold parameter with mean $\theta + \frac{\sigma}{1-\eta}$ and infinite variance. The probability $P_{\text{in}}(0)$ that a node is a root is then $e^{-\lambda}$ and $\varphi_{\text{in}}(0)/\sum_{z=0}^{N-1} \varphi_{\text{n}}(z)$ for the Poisson and generalized Pareto distributions, respectively, so that for all $\bar{k} \geq 1$ the generated graph was endowed with a G_{SCC}.

We tested our ability to predict the number of pinned nodes $m^\star$ required to induce the explosive phase transition on a set of randomly generated and scale-free networks of 1 million nodes, where we varied the average degree $\bar{k}$ in the interval $[10^0\ \ 10^3]$ so that for all $\bar{k}$ the generated graph was endowed with a G_{SCC}. Namely, for Poisson degree distributions, we vary the parameter $\lambda = \bar{k}$ ranging in logarithmic scale between 10^0 and 10^3, whereas, for scale-free distributions, we select $\theta = 0, \eta = 0.5$ and σ modulated so that $\bar{k}$ approximately ranges in logarithmic scale between 10^0 and 10^3.

Fig. 4 shows that our estimate $\hat{m}^\star$ from Eq. (15) is in excellent agreement with $m^\star$. Moreover, we can note that this threshold peaks at $\bar{k} = 1.5$ and $\bar{k} = 2.5$ for random and scale-free graphs, respectively, to then approach 0. In random graphs, as $\bar{k}$ is further increased, the network then becomes strongly connected thus pinning one R_{SCC} is sufficient to control the entire of the network (this occurs when the $\bar{k}$ approaches 5). In scale-free networks, instead, $\hat{m}^\star$ reduces at a much slower pace with $\bar{k}$ because of the presence of a relevant fraction of low-degree nodes that would still not belong to the G_{SCC}.

For the same two sets of topologies, for each degree distribution type and selection of the average degree, we compute the lower and upper bound, $\underline{P}$ from (25) and $\overline{P}$ from (21) respectively, of the expected fraction of nodes that we cannot control. These bounds are then compared in Fig. 5 with the observed fraction of nodes of G_{WCC} that we are not able to control, that is, $|\bar{Q}(m^\star)|/|G_{\text{WCC}}|$. We notice how the bounds correctly hold for all $\bar{k}$ and distribution type, and that both $\underline{P}$ and upper bound $\overline{P}$ converge to $|\bar{Q}(m^\star)|/|G_{\text{WCC}}|$ when $\bar{k}$ increases, even though at a slower pace in scale-free compared to the case of the Poisson random degree distributions.

Next, we retrieved three large real digraphs of about one million nodes from the network repository in [22] and performed the same simulations made for the synthetic dataset. From Table 1, we can appreciate how well the estimation (17) of $m^\star$ works also for real topologies where the assumption on the statistical independence of the in- and out-degree may not hold. In 2 out of 3 real networks the estimation error is 0, and in all the cases, is never larger than 12%. The lower and upper bounds $\underline{P}$ and $\overline{P}$ capture the fact that the fraction of observed nodes that we cannot control is small. For the same reason, though, the approximations considered in the estimation of the bounds become dominant, limiting their accuracy.

5. Conclusion

Percolation in graphs with an arbitrary degree distribution is a well-known phenomenon, as well as pinning synchronizability is in complex networks. This work aims to bridge this two established research avenues in network science, and explain, with the sole knowledge of the networks in- and out-degree distributions, how pinning synchronization can be induced by the presence of a percolation cluster, a giant strongly connected component. Leveraging tools from the generative functions' theory, we analytically and numerically illustrate that, when the network percolates and a giant component appears, the phase transition in the number of controllable nodes as we increase the number of control signals becomes explosive. To do so, we first identify the class of network dynamical systems for which this result hold, by extending the classical definition of class II master stability function to the case of controlled networks. Then, for this class of networks, we analytically estimate the threshold in the number of controlled nodes that, when attained, determines the onset of the explosive phase transition. Finally, we also provide an upper and lower bound on the fraction of nodes that we are still unable to control when the transition takes place. The analytical findings are then corroborated by extensive numerical analyses on large synthetic network (up to approximately one million nodes), and by a validation on select real networks with size of the order of one million nodes, which show an excellent agreement between the theoretical prediction and the actual transition threshold.

Future works could be devoted to investigate how this analysis would extend when we go beyond pairwise interactions, and consider that the network systems may exhibit group interactions that cannot be decomposed as combinations of pairwise ones. To this aim, one could leverage the recent results on percolation in hypergraphs [34,35], and study the possible implications on control of networks with higher-order interaction, to explain whether and when explosive transitions in the number of controlled nodes can be expected. Richer phenomena due to the presence of higher-order interactions may also be expected. Another research avenue that could be considered is the impact of alternative control strategies, other than standard, proportional pinning control, and in particular when the coupling strengths or the network topology change over time [36,37].

CRediT authorship contribution statement

Camilla Ancona: Writing – review & editing, Writing – original draft, Visualization, Software, Investigation, Formal analysis. **Fabio Della Rossa:** Writing – review & editing, Software. **Francesco Lo Iudice:** Writing – review & editing, Writing – original draft, Supervision, Investigation, Formal analysis, Conceptualization. **Pietro De Lellis:** Writing – review & editing, Writing – original draft, Supervision, Investigation, Formal analysis, Conceptualization.

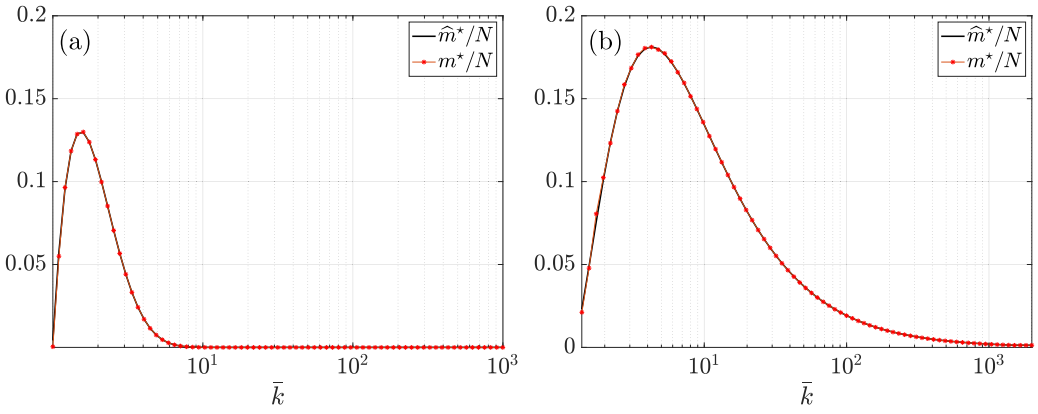

Fig. 4. Comparing the critical fraction $m^\star/N$ of pinned nodes that triggers an explosive phase transition (the red stars) with the analytic prediction $\widehat{m}^\star$ (black solid lines). In panel (a), we consider random networks and, in panel (b), scale-free networks, both with average degree $\bar{k}$ ranging from 1 to 1000. (For interpretation of the references to color in this figure legend, the reader is referred to the web version of this article.)

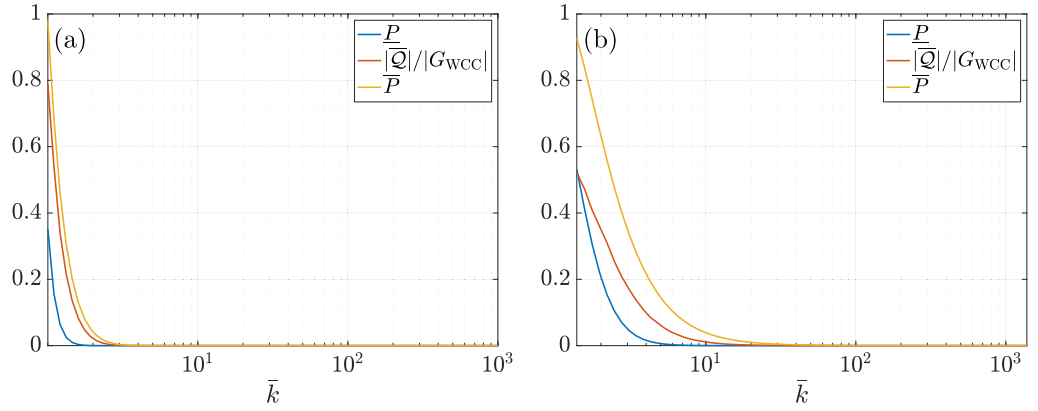

Fig. 5. Computation of the lower $\underline{P}$ from (25) and upper bound $\overline{P}$ (21) in blue and yellow respectively, of the expected fraction of nodes that we cannot control $|\bar{\mathcal{Q}}(m^\star)|/|G_{\mathrm{WCC}}|$ in red. In panel (a), we validate the prediction for random networks, whereas, and in panel (b), we validate it for scale-free networks. (For interpretation of the references to color in this figure legend, the reader is referred to the web version of this article.)

Table 1
Predicting the threshold of $m^\star$ for real directed networks. The first column reports the tag for the network used in [22], the second to the network size, the third column the average degree $\bar{k}$, the fourth the estimate $\widehat{m}^\star$ according to (17), and the fifth the actual threshold $m^\star$. The last three columns report the lower bound $\underline{P}$, the observed fraction of nodes that we are not able to control $|\bar{\mathcal{Q}}(m^\star)|/|G_{\mathrm{WCC}}|$, and the upper bound $\overline{P}$, respectively.

Network	N	$\bar{k}$	$\widehat{m}^\star$	$m^\star$	$\underline{P}$	$\lvert\bar{\mathcal{Q}}\rvert/\lvert G_{\mathrm{WCC}}\rvert$	$\overline{P}$
atmosmodl	1 489 752	0.5651	39 203	39 203	0.0523	0	0.0572
ca-IMDB	896 308	4.2200	3	3	1.49×10^{-11}	7.81×10^{-6}	2.23×10^{-6}
flickr	2 406 556	17.3216	57 424	51 561	1.98×10^{-8}	0.0325	8.31×10^{-7}

Declaration of competing interest

The authors declare that they have no known competing financial interests or personal relationships that could have appeared to influence the work reported in this paper.

Data availability

Data will be made available on request.

Acknowledgments

This study was carried out within the 2022K8EZBW "Higher-order interactions in social dynamics with application to monetary networks" project – funded by European Union – Next Generation EU within the PRIN 2022 program (D.D. 104 - 02/02/2022 Ministero dell'Università e della Ricerca). This manuscript reflects only the authors' views and opinions and the Ministry cannot be considered responsible for them.

References

[1] Boccaletti S, Latora V, Moreno Y, Chavez M, Hwang D-U. Complex networks: Structure and dynamics. Phys Rep 2006;424(4–5):175–308.
[2] Albert R, Barabási A-L. Statistical mechanics of complex networks. Rev Modern Phys 2002;74(1):47.
[3] Rosvall M, Bergstrom CT. Maps of random walks on complex networks reveal community structure. Proc Natl Acad Sci 2008;105(4):1118–23.
[4] Dörfler F, Bullo F. Synchronization in complex networks of phase oscillators: A survey. Automatica 2014;50(6):1539–64.
[5] Strogatz SH. Exploring complex networks. Nature 2001;410(6825):268–76.
[6] Echenique P, Gómez-Gardenes J, Moreno Y. Dynamics of jamming transitions in complex networks. Europhys Lett 2005;71(2):325.
[7] Ginsparg P. First and second order phase transitions in gauge theories at finite temperature. Nuclear Phys B 1980;170(3):388–408.
[8] Boccaletti S, Almendral J, Guan S, Leyva I, Liu Z, Sendiña-Nadal I, Wang Z, Zou Y. Explosive transitions in complex networks' structure and dynamics: Percolation and synchronization. Phys Rep 2016;660:1–94.
[9] D'Souza RM, Gómez-Gardenes J, Nagler J, Arenas A. Explosive phenomena in complex networks. Adv Phys 2019;68(3):123–223.
[10] Zhang X, Zou Y, Boccaletti S, Liu Z. Explosive synchronization as a process of explosive percolation in dynamical phase space. Sci Rep 2014;4(1):5200.

[11] Moreno Y, Pacheco AF. Synchronization of kuramoto oscillators in scale-free networks. Europhys Lett 2004;68(4):603.
[12] Gómez-Gardenes J, Gómez S, Arenas A, Moreno Y. Explosive synchronization transitions in scale-free networks. Phys Rev Lett 2011;106(12):128701.
[13] Kuramoto Y. Chemical oscillations, waves, and turbulence. Springer-Verlag; 1984.
[14] Liu Y-Y, Barabási A-L. Control principles of complex systems. Rev Modern Phys 2016;88(3):035006.
[15] D'Souza RM, di Bernardo M, Liu Y-Y. Controlling complex networks with complex nodes. Nat Rev Phys 2023;5(4):250–62.
[16] Liu X, Pan L, Stanley HE, Gao J. Controllability of giant connected components in a directed network. Phys Rev E 2017;95(4):042318.
[17] Wang XF, Chen G. Pinning control of scale-free dynamical networks. Phys A 2002;310(3–4):521–31.
[18] Della Rossa F, De Lellis P. Synchronization and pinning control of stochastic coevolving networks. Annu Rev Control 2022;53:147–60.
[19] DeLellis P, Garofalo F, Lo Iudice F. The partial pinning control strategy for large complex networks. Automatica 2018;89:111–6.
[20] Lu W, Chen T. New approach to synchronization analysis of linearly coupled ordinary differential systems. Physica D 2006;213(2):214–30.
[21] Davydov A, Jafarpour S, Bullo F. Non-euclidean contraction theory for robust nonlinear stability. IEEE Trans Autom Control 2022;67(12):6667–81.
[22] Rossi RA, Ahmed NK. The network data repository with interactive graph analytics and visualization. In: AAAI. 2015, p. 4292–3, URL http://networkrepository.com.
[23] Boccaletti S, De Lellis P, del Genio C, Alfaro-Bittner K, Criado R, Jalan S, Romance M. The structure and dynamics of networks with higher order interactions. Phys Rep 2023;1018:1–64.
[24] Nishikawa T, Motter AE. Synchronization is optimal in nondiagonalizable networks. Phys Rev E 2006;73(6):065106.
[25] Della Rossa F, Liuzza D, Lo Iudice F, De Lellis P. Emergence and control of synchronization in networks with directed many-body interactions. Phys Rev Lett 2023;131(20):207401.
[26] Gambuzza LV, Di Patti F, Gallo L, Lepri S, Romance M, Criado R, Frasca M, Latora V, Boccaletti S. Stability of synchronization in simplicial complexes. Nature Commun 2021;12(1):1255.
[27] Dorogovtsev SN, Mendes JFF, Samukhin AN. Giant strongly connected component of directed networks. Phys Rev E 2001;64(2):025101.
[28] Tarjan R. Depth-first search and linear graph algorithms. SIAM J Comput 1972;1(2):146–60.
[29] Wilf HS. Algorithms and complexity. In: Summer. 1994, p. 1.
[30] Newman ME, Strogatz SH, Watts DJ. Random graphs with arbitrary degree distributions and their applications. Phys Rev E 2001;64(2):026118.
[31] Barabási A-L. Network science. Phil Trans R Soc A 2013;371(1987):20120375.
[32] Yates RD, Goodman DJ. Probability and stochastic processes: a friendly introduction for electrical and computer engineers. John Wiley & Sons; 2014.
[33] Kotz S, Nadarajah S. Extreme value distributions: theory and applications. World Scientific; 2000.
[34] Pan X, Zhou J, Zhou Y, Boccaletti S, Bonamassa I. Robustness of interdependent hypergraphs: A bipartite network framework. Phys Rev Res 2024;6(1):013049.
[35] Bianconi G, Dorogovtsev SN. Theory of percolation on hypergraphs. Phys Rev E 2024;109(1):014306.
[36] Turci L, De Lellis P, Macau E, di Bernardo M, Simões M. Adaptive pinning control: A review of the fully decentralized strategy and its extensions. Eur Phys J Spec Top 2014;223:2649–64.
[37] DeLellis P, di Bernardo M, Porfiri M. Pinning control of complex networks via edge snapping. Chaos 2011;21(3).